

lncRNA PVT1 modulates NLRP3-mediated pyroptosis in septic acute kidney injury by targeting miR-20a-5p

LONG-TIAN DENG, QIAN-LU WANG, CAN YU and MIN GAO

Department of Critical Care Medicine, The Third Xiangya Hospital,
Central South University, Changsha, Hunan 410013, P.R. China

Received June 22, 2020; Accepted December 15, 2020

DOI: 10.3892/mmr.2021.11910

Abstract. Acute kidney injury (AKI) is the most common complication of sepsis. The current incidence of sepsis is high (0.3% of total population) worldwide, and septic AKI may cause death in patients. Long non-coding (lnc)RNAs serve important roles in the pathogenesis of AKI. Therefore, the present study investigated the mechanism underlying lncRNA plasmacytoma variant translocation 1 (PVT1)-mediated regulation of pyroptosis in septic AKI. Septic kidney injury was induced in mice using the caecal ligation and puncture method, and lipopolysaccharide (LPS)-induced HK-2 cell models were also established. Haematoxylin-eosin staining was performed to assess pathological alterations of kidney tissues in the mice. The levels of IL-1 β , IL-18 and lactate dehydrogenase were determined by conducting ELISAs. Reverse transcription-quantitative PCR was used to detect the expression levels of PVT1 and microRNA (miR)-20a-5p. To assess pyroptosis, the protein expression levels of nucleotide-binding oligomerization domain-like receptor protein 3 (NLRP3), IL-1 β , IL-18, apoptosis-associated speck-like protein containing a CARD and cleaved caspase-1 were measured via western blotting. Flow cytometry was performed to assess the rate of cell pyroptosis. Dual luciferase reporter assays were used to assess the binding relationships of PVT1/miR-20a-5p and miR-20a-5p/NLRP3. PVT1 expression was significantly increased, whereas miR-20a-5p expression was significantly decreased in sepsis model mice and LPS-induced HK-2

cells compared with sham mice and control HK-2 cells, respectively. PVT1 knockdown significantly suppressed cell pyroptosis and downregulated the expression of inflammatory factors in LPS-induced HK-2 cells. The results also indicated that PVT1 served as a sponge of miR-20a-5p, and miR-20a-5p directly targeted NLRP3. miR-20a-5p knockdown significantly promoted LPS-induced cell pyroptosis. Moreover, PVT1 knockdown inhibited LPS-induced cell pyroptosis by targeting the miR-20a-5p/NLRP3 signalling pathway. The results of the present study suggested that PVT1 modulated NLRP3-mediated pyroptosis in septic AKI by targeting miR-20a-5p, which might suggest significant potential therapeutic targets for septic AKI.

Introduction

Septicaemia is a life-threatening disease in which a patient's own tissues and organs are damaged as a result of the patient's response to infection (1). Sepsis is typically associated with multiple organ failure, and acute kidney injury (AKI) is the most common potentially fatal complication of sepsis (2). AKI caused by sepsis is a serious medical problem in the intensive care unit, with a mortality rate as high as 50-70% in a study of 54 hospitals in 23 countries (3). However, the pathophysiological mechanisms underlying septic AKI are not completely understood, which limits the development of effective therapeutic strategies. Therefore, exploring the molecular mechanism underlying the occurrence and development of septic AKI is important as it will aid with the identification of novel targets and directions for the treatment of septic AKI.

Long non-coding (lnc)RNAs do not encode proteins and are >200 nucleotides in length (4). Increasing evidence demonstrates that lncRNAs serve important roles in the pathogenesis of AKI (5,6). lncRNA plasmacytoma variant translocation 1 (PVT1) has been reported to be highly expressed in several human diseases, including septic AKI (5,7). Kidney tissues of lipopolysaccharide (LPS)-induced AKI mice displayed high PVT1 and inflammatory factor expression levels, but PVT1 knockdown alleviated cellular inflammation in the kidney tissues of sepsis model mice (5). However, the molecular mechanism underlying PVT1 in septic AKI requires further investigation.

MicroRNAs (miRNAs/miRs) are endogenous short RNAs (21-25 nucleotides) that post-transcriptionally regulate gene

Correspondence to: Dr Min Gao, Department of Critical Care Medicine, The Third Xiangya Hospital, Central South University, 138 Tongzipo Road, Changsha, Hunan 410013, P.R. China
E-mail: gmgaomin79@163.com

Abbreviations: AKI, acute kidney injury; PVT1, plasmacytoma variant translocation 1; lncRNAs, long non-coding RNAs; miRNA/miR, microRNA; NLRP3, nucleotide-binding oligomerization domain-like receptor protein 3; UTR, untranslated region; ASC, apoptosis-associated speck-like protein containing a CARD; H&E, haematoxylin and eosin

Key words: sepsis, lncRNA PVT1, acute kidney injury, miR-20a-5p, NLRP3, pyroptosis

expression (8). miRNAs are involved in almost all biological processes, including development, cell differentiation and proliferation, metabolism and apoptosis (9). A previous study suggested that miR-20a-5p serves an important role in AKI (10). miR-20a-5p downregulation was detected in kidneys after ischaemic injury and in HK-2 cells under hypoxic conditions, and miR-20a-5p modulated autophagy by suppressing autophagy related 16 like 1 (11). However, the specific mechanism underlying miR-20a-5p in septic AKI is not completely understood. miRNAs bind to the 3'-untranslated region (UTR) of the target gene mRNA, causing mRNA degradation and inhibiting protein translation (8). Thus, it is necessary to further examine the effect of miR-20a-5p on downstream gene expression and the specific molecular mechanism of its role in sepsis.

Increasing evidence suggests that the NLRP3 inflammasome serves an important role in the pathogenesis of AKI (12-14). Once activated, the NLRP3 inflammasome induces the maturation and release of proinflammatory cytokines, including IL-1 β and IL-18, which serve important roles in promoting the inflammatory process (10). Pyroptosis, an emerging intrinsic cell death mechanism, is associated with the inflammatory response (15). Therefore, the present study further investigated the role of the NLRP3 inflammasome in mediating pyroptosis in AKI.

In the present study, the molecular mechanism underlying PVT1 in septic AKI was investigated and the effect of miR-20a-5p/NLRP3 in inflammasome of septic AKI was clarified. This will provide new ideas for the prevention and treatment of septic AKI.

Materials and methods

Materials. DMEM, FBS and nutrient mixture F-12 were purchased from Gibco (Thermo Fisher Scientific, Inc). LPS and formalin were obtained from Sigma-Aldrich (Merck KGaA). The human/mouse IL-1 β and IL-18 ELISA kits were purchased from Sigma-Aldrich (Merck KGaA). The endonucleases *Xho*I and *Hind*III, Lipofectamine[®] 3000 and TRIzol[®] reagent were obtained from Invitrogen (Thermo Fisher Scientific, Inc.). The Cytoplasmic & Nuclear RNA Purification kit was obtained from Norgen Biotek Corp. Anti-NLRP3, anti-IL-1 β , anti-IL-18, anti-apoptosis-associated speck-like protein containing a CARD (ASC), anti-cleaved gasdermin D (GSDMD), anti-cleaved gasdermin E (GSDME) and anti-caspase-11 primary antibodies, and the HRP-conjugated secondary antibody were purchased from Abcam. The anti-cleaved caspase-1 primary antibody was purchased from Cell Signaling Technology, Inc. The haematoxylin and eosin (H&E) staining kit was purchased from Wuhan Boster Biological Technology, Ltd. The BCA kit, lactate dehydrogenase (LDH)-cytotoxicity assay kit and ECL reagent were obtained from Beyotime Institute of Biotechnology. The ReverTra Ace[™] qPCR RT kit and SYBR Green PCR kit were purchased from Toyobo Life Science. The FLICA 660 *in vitro* active caspase-1 detection kit and PI solution were obtained from ImmunoChemistry Technologies, LLC. The pcDNA3.1 vector, small interfering RNA (si)NLRP3, siNC, shPVT1 and shNC were purchased from Shanghai GenePharma Co., Ltd. The firefly luciferase reporter plasmid pGL3-Basic was obtained from Promega Corporation.

Mouse feeding and construction of the sepsis model. A total of 10 male C57/BL6 mice (age, 6 weeks; weight, 25 \pm 3 g) were purchased from Hunan SJA Laboratory Animal Co., Ltd. and fed in separate cages. Mice were housed at 22 \pm 1 $^{\circ}$ C and 60% humidity with 12-h light/dark cycles, and free access to water and food. Mice were randomly divided into two groups (n=5 per group): i) Sham operation (sham); and ii) Sepsis model (sepsis). All surgical procedures were performed under sterile conditions. The sham group were only subjected to open abdominal cavity operations, excluding the caecal ligation and puncture. Mice were anaesthetized by the intraperitoneal injection of 150 mg/kg ketamine and 10 mg/kg xylazine. Subsequently, an incision was made in the mouse midline. The caecum was isolated and ligated distal to the ileocecal valve using 3/0 silk sutures. The caecum content was brought into contact with the peritoneum by opening two holes with a needle distal from the mesentery to the opposite side. The abdominal incision was then closed with two layers of sterile 4/0 synthetic absorbable sutures. Following induction of deep anaesthesia by inhalation of 5% isoflurane (Merck Sharp & Dohme-Hoddesdon), mice were euthanized by cervical dislocation. Mouse blood (0.5 ml) was collected by inserting a syringe into the heart. After centrifugation (1,000 x g, 5 min at room temperature), serum was collected for detection of creatinine and urea nitrogen using a Beckman AU 480 automatic analyser (Beckman Coulter, Inc.). All procedures related to animal experiments were reviewed and approved by The Third Xiangya Hospital of Central South University [approval no. LLSC (LA)2018-030].

Cell culture and model building. The HK-2 human tubular epithelial cell line was obtained from The Cell Bank of Type Culture Collection of The Chinese Academy of Sciences. HK-2 cells were cultured in DMEM/Nutrient Mixture F-12 (1:1) supplemented with 10% FBS at 37 $^{\circ}$ C with 5% CO₂. To induce the cell sepsis model, HK-2 cells were treated with 2 μ g/ml LPS for 8 h at 37 $^{\circ}$ C. The control cells did not receive any treatment.

H&E staining. Mouse kidneys were fixed overnight in 10% formalin at 4 $^{\circ}$ C and embedded in paraffin. Kidney tissues were sliced into 4- μ m thick sections using an automatic microtome (Leica Microsystems GmbH). Sections were dewaxed using xylene (I and II; 10 min per solution), rehydrated using a descending alcohol series (100, 95, 80 and 70%; 5 min per solution), washed with running tap water and stained with Mayer's haematoxylin for 4 min at room temperature. Following washing in running tap water, sections were dehydrated in ethanol (85 and 95%; 5 min per solution), stained with eosin solution for 5 min at room temperature and then rinsed in tap water to remove excess stain. Subsequently, sections were rapidly dehydrated using graded ethanol (80, 95 and 100%) in xylene and sealed using neutral gum. Stained sections were observed using an inverted fluorescence microscope at x100 magnification (Olympus Corporation).

Plasmid constructs and transfection. Plasmid DNA-encoding PVT1 was constructed by inserting the cDNA clone of PVT1 into a pcDNA3.1 vector (Invitrogen; Thermo Fisher Scientific, Inc.). miR-20a-5p mimic (5'-UAAAGU GCUUAUAGUGCAGGUAG-3'), mimic NC (5'-UUC UCCGAACGUGUCACGUTT-3'), miR-20a-5p inhibitor

(5'-CUACCUGCACUAUAAGCACUUUA-3') and inhibitor NC (5'-CAGUACUUUUGUGUAGUACAA-3') were synthesized by Sangon Biotech Co., Ltd. Cells (1×10^5 cells/well) were transfected with pcDNA3.1-PVT1 (1 μ g), pcDNA3.1-NC (1 μ g), siNLRP3 (50 nM), siNC (non-targeting control; 50 nM), shPVT1 or shNC (BLOCK-iT™ shRNA Vectors; Thermo Fisher Scientific, Inc.; NC, non-targeting control; 50 nM), miR-20a-5p mimic or NC (100 nM), miR-20a-5p inhibitor or NC (100 nM) using Lipofectamine 3000 according to the manufacturer's instructions at 37°C for 6 h. Cells were harvested for further experiments after 24 h.

Reverse transcription-quantitative PCR (RT-qPCR). Total RNA was extracted using TRIzol reagent from mice kidney tissues and HK-2 cells. Total RNA was reverse transcribed into cDNA using a ReverTra Ace™ qPCR RT kit according to the manufacturer's protocol. Subsequently, qPCR was performed using a Mastercycler RealPlex4 (Eppendorf) with the SYBR Green PCR kit. The following thermocycling conditions were used for qPCR: Initial denaturation at 95°C for 5 min; followed by 40 cycles at 95°C for 15 sec, 60°C for 30 sec and 72°C for 30 sec. The following primers were used for qPCR: PVT1 forward, 5'-AAAACGGCAGCAGGAAATGT-3' and reverse, 5'-CCTCGGTCCACGCCTTCCCTC-3'; miR-20a-5p forward, 5'-UAAAGUGCUUAUAGUGCAGGUAG-3' and reverse, 5'-CUACCUGCACUAUAAGCACUUUA-3'; NLRP3 forward, 5'-GATCTTCGCTGCGATCAACAG-3' and reverse, 5'-CGTGCATTATCTGAACCCAC-3'; U6 forward, 5'-CTC GCTTCGGCAGCACA-3 and reverse, 5'-AACGCTTCAGAA TTTGCCT-3'; and GAPDH forward, 5'-GAGTCAACGGAT TTGGTTCGTT-3' and reverse, 5'-TTGATTTTGGAGGGA TCTCG-3'. Cytoplasmic and nuclear RNAs were isolated using Cytoplasmic & Nuclear RNA Purification kit (Norgen Biotek Corp.) according to the supplier's instructions, and measured via RT-qPCR. The nuclear and cytoplasmic RNAs were normalized to U6 and GAPDH, respectively. miRNA and mRNA expression levels were quantified using the $2^{-\Delta\Delta C_q}$ method (16) and normalized to the internal reference genes U6 and GAPDH, respectively.

Pyroptosis detection via flow cytometry. Cells were seeded (2×10^5 cells/well) into 6-well plates. Cells were harvested and washed with PBS. To identify pyroptotic cells, cells were stained with FLICA 660-YVAD-FMK (FLICA 660 *in vitro* active caspase-1 Detection kit) and PI according to the manufacturer's protocol. Subsequently, cells were analysed using a BD LSRFortessa Cell Analyser (BD Biosciences) and pyroptotic cells were analysed using FlowJo software V7.6.5 (FlowJo, LLC). Pyroptotic cells were defined as active caspase-1-PI double-positive cells.

ELISAs. The levels of IL-1 β and IL-18 were determined using human/mouse IL-1 β and IL-18 ELISA kits according to the manufacturer's protocol, respectively. Blood samples were centrifuged at 1,000 \times g for 10 min at 4°C to collect serum. Subsequently, 50 μ l diluted sample (containing 10 μ l serum and 40 μ l sample dilution, or 30 μ l cell supernatant and 20 μ l sample dilution) and 100 μ l HRP-conjugated secondary antibody were added to each well of the antibody-coated plate. Following incubation for 1 h at 37°C in the dark, the liquid was

removed from the microtiter plate. Each well was washed five times with washing solution. Subsequently, 50 μ l reaction solution was added to each well and incubated for 30 min at room temperature. Then, 50 μ l stop solution was added to each well. The absorbance of each well was measured at a wavelength of 450 nm using a microplate reader.

LDH secretion in cell samples was measured using an LDH-cytotoxicity assay kit according to the manufacturer's instructions.

Plasmid vector construction and dual luciferase reporter assay. starBase (starbase.sysu.edu.cn), an online target prediction website, was used to predict the base sequence of the binding site between PVT1 and miR-20a-5p. The wild-type (WT) 3'UTR sequence of PVT1 was cloned into the firefly luciferase reporter plasmid pGL3-Basic (Promega Corporation) following *Xho*I and *Hind*III restriction enzyme digestion. After site-directed mutation of the potential complementary binding site, the pGL3 vector was double-enzyme digested by *Xho*I and *Hind*III. The mutant (MUT) fragment was inserted into the vector to construct a mutant recombinant dual luciferase reporter vector. Cells (1×10^5 cells/well) were co-transfected with PVT1-WT (2 μ g) or PVT1-MUT (2 μ g) and mimic NC (50 nM) or miR-20a-5p mimic (50 nM) using Lipofectamine 3000 at 37°C for 6 h according to the manufacturer's instructions. The same protocol (the 3'UTR sequence of NLRP3 was used to instead of PVT1) was used for the dual luciferase reporter assay for the investigation of the interaction between miR-20a-5p and NLRP3. Luciferase activity was detected using a Dual-Glo luciferase assay kit (Promega Corporation) after the cells were cultured for 48 h. The firefly luciferase activity was normalized to *Renilla* luciferase activity.

Total protein extraction and western blotting. Total protein was isolated from mice kidney tissues and cells using RIPA (cat. no. R0278; Sigma-Aldrich; Merck KGaA) mixed with 1% protease inhibitor and phosphorylase inhibitor. Protein concentrations were determined using a BCA kit. Lysate samples (25 μ g/lane) were separated using 12% SDS-PAGE and then transferred to a PVDF membrane (MilliporeSigma). The membrane was blocked with 5% non-fat milk powder at room temperature for 2 h. Subsequently, the membranes were incubated overnight at 4°C with primary antibodies targeted against: NLRP3 (1:1,000; cat. no. ab263899), IL-1 β (1:1,000; cat. no. ab234437), IL-18 (1:1,000; cat. no. ab207324), ASC (1:1,000; cat. no. ab151700), cleaved caspase-1 (1:1,000; cat. no. 89332), cleaved GSDMD (1:1,000; cat. no. ab227821), cleaved GSDME (1:1,000; cat. no. ab222408), caspase-11 (1:1,000; cat. no. ab180673) and β -actin (Sigma-Aldrich; Merck KGaA; 1:10,000; cat. no. A1978). After washing with 0.1% Tween-20 in PBS-T (Sangon Biotech Co., Ltd.), the membranes were incubated at room temperature for 1 h with the corresponding HRP-conjugated secondary antibody (Boster Biological Technology Co, Ltd.; 1:10,000; cat. no. BA1056). Protein bands were visualized using ECL reagent and a GEL imaging system (Bio-Rad Laboratories, Inc.). Protein expression was semi-quantified using Quantity One software V4.3 (Bio-Rad Laboratories, Inc.) with β -actin as the loading control.

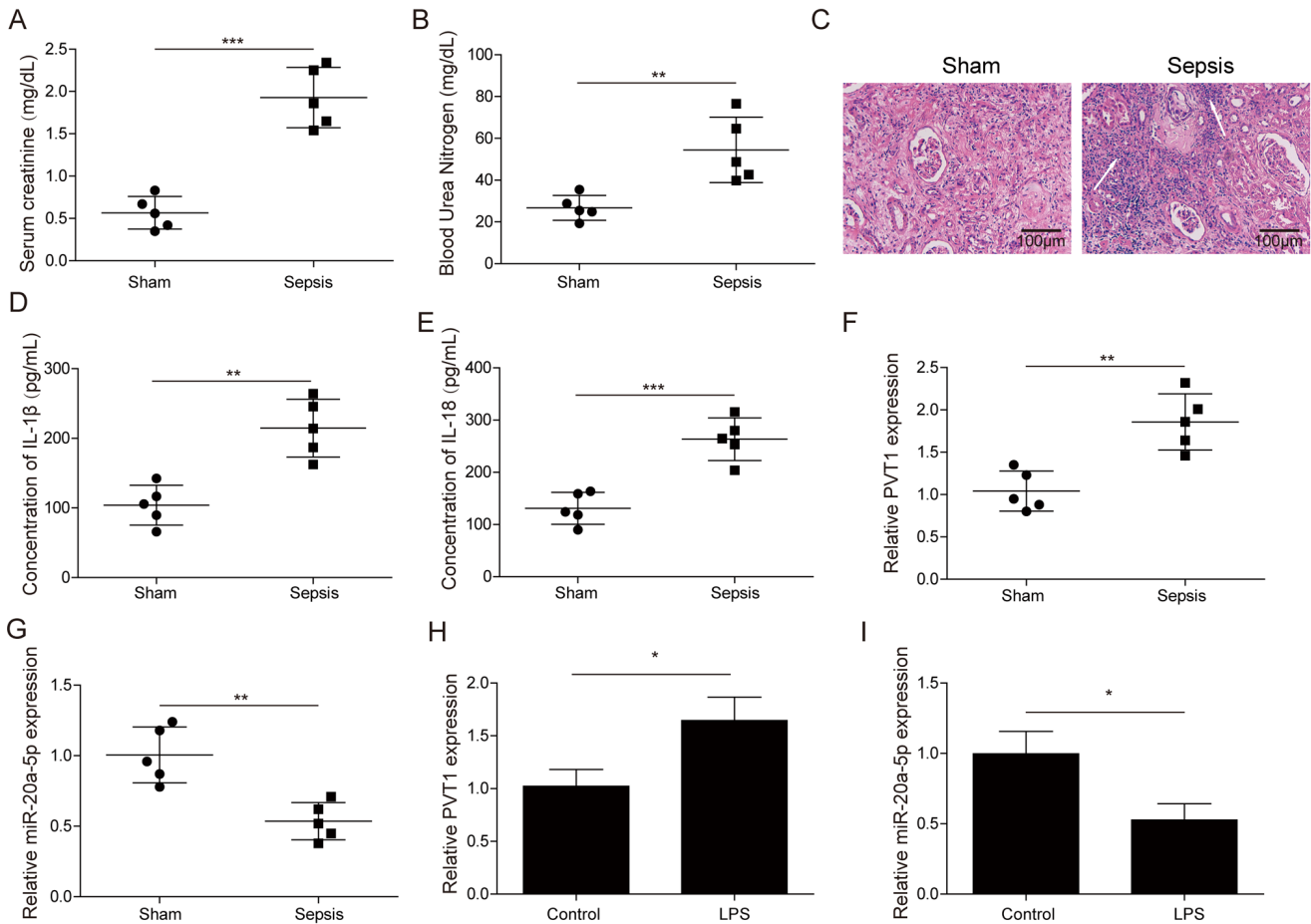


Figure 1. PVT1 expression is increased, whereas miR-20a-5p expression is decreased in sepsis model mice and LPS-induced HK-2 cell models. Serum (A) creatinine and (B) urea nitrogen levels were detected using a Beckman Automatic Analyser. (C) Haematoxylin and eosin staining of kidney tissues. Serum (D) IL-1 β and (E) IL-18 levels were detected by performing ELISAs. (F) PVT1 and (G) miR-20a-5p expression levels in kidney tissues were detected via RT-qPCR. (H) PVT1 and (I) miR-20a-5p expression levels in HK-2 cells were determined via RT-qPCR. * $P < 0.05$, ** $P < 0.01$ and *** $P < 0.001$. PVT1, plasmacytoma variant translocation 1; miR, microRNA; LPS, lipopolysaccharide; RT-qPCR, reverse transcription-quantitative PCR.

Statistical analysis. All experiments were performed three times. Data are presented as the mean \pm SD. Statistical analyses were performed using GraphPad Prism 8.0 software (GraphPad Software, Inc.). Comparisons between two groups were analysed using the unpaired Student's t-test. Comparisons among multiple groups were analysed using one-way ANOVA followed by Tukey's post hoc test. $P < 0.05$ was considered to indicate a statistically significant difference.

Results

PVT1 expression is increased, whereas miR-20a-5p expression is decreased in sepsis model mice and LPS-induced HK-2 cell models. First, a septic mouse model was constructed using the caecal ligation and puncture method (17) (the detailed steps are outlined in the Materials and methods section). The serum levels of creatinine and urea nitrogen were significantly increased in the sepsis group compared with the sham group (Fig. 1A and B). Histopathological characteristics of renal tubules, including the formation of transparent moulds, cavitation, extensive necrosis and exfoliation of the basement membrane, were observed in the sepsis group by H&E staining of the kidney (Fig. 1C). Moreover, the serum levels of IL-1 β and IL-18 were significantly upregulated in the

sepsis group compared with the sham group (Fig. 1D and E). IL-1 β and IL-18 protein expression levels displayed similar trends, as demonstrated via western blotting (Fig. S1). In addition, the protein expression levels of NLRP3, ASC and cleaved-caspase 1 were significantly increased in the sepsis group compared with the sham group (Fig. S1). The aforementioned results suggested that cell pyroptosis might occur in the kidneys of sepsis model mice. Moreover, the results demonstrated that the septic mouse model was successfully constructed. Compared with the sham group, PVT1 expression levels were significantly upregulated, and miR-20a-5p expression levels were significantly downregulated in the sepsis group (Fig. 1F and G). A similar trend was observed in LPS-induced HK-2 cells compared with control HK-2 cells (Fig. 1H and I). Collectively, the results suggested that PVT1 was upregulated, whereas miR-20a-5p was downregulated in sepsis model mice and LPS-induced HK-2 cells.

PVT1 knockdown reduced NLRP3-mediated pyroptosis in LPS-induced HK-2 cells. To further investigate the effect of PVT1 on cell pyroptosis, PVT1 expression was knocked down in LPS-induced HK-2 cells. PVT1 expression levels were significantly increased in the LPS group compared with the control group, but were significantly decreased by shPVT1

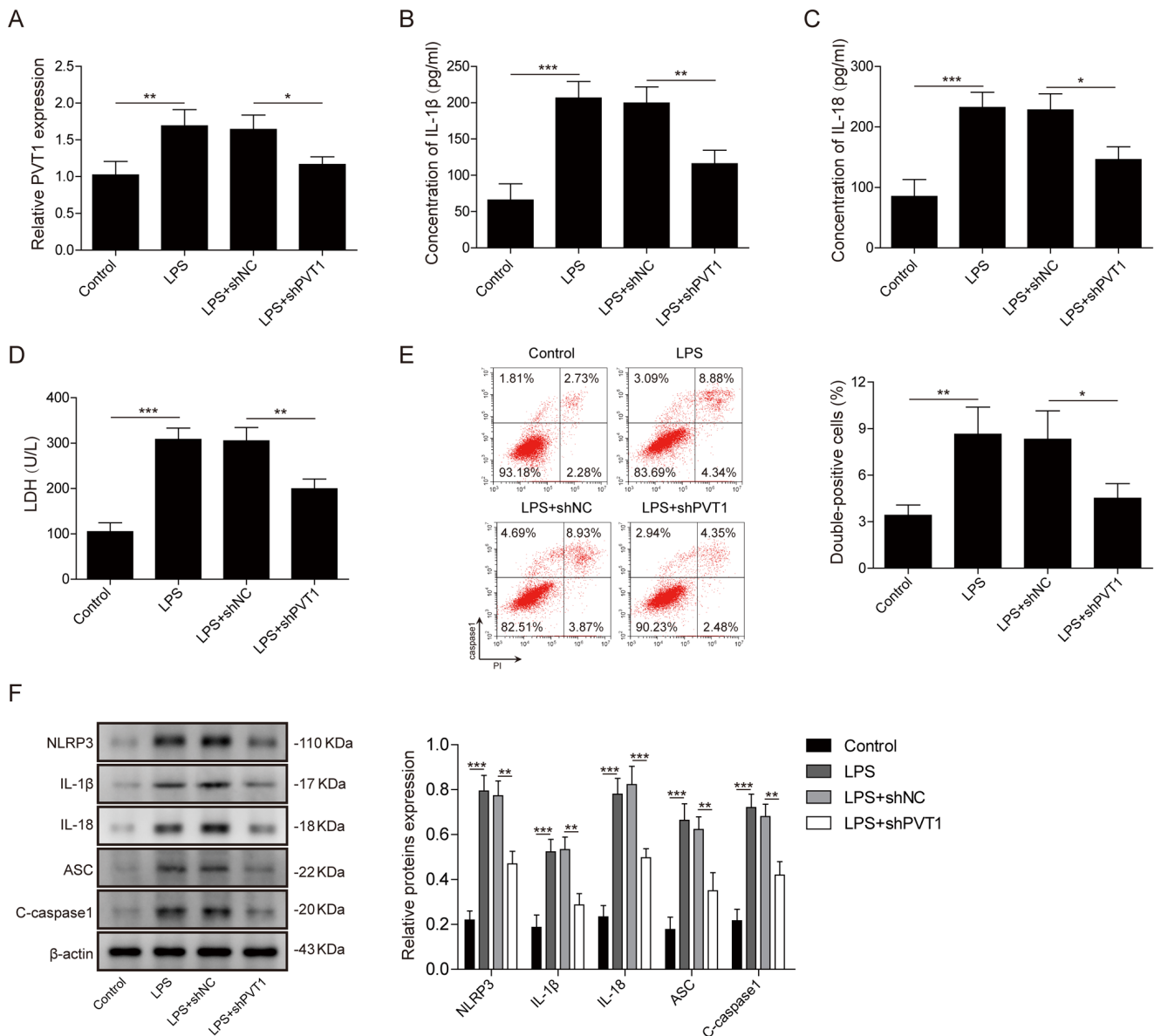


Figure 2. PVT1 knockdown reduces NLRP3-mediated pyroptosis in LPS-induced HK-2 cells. (A) PVT1 expression in HK-2 cells was detected via reverse transcription-quantitative PCR. (B) IL-1 β and (C) IL-18 levels in HK-2 cells were detected by performing ELISAs. (D) LDH secretion was measured using an LDH cytotoxicity assay kit. (E) Cell pyroptosis was detected via flow cytometry. (F) NLRP3, IL-1 β , IL-18, ASC and cleaved caspase-1 protein expression levels were determined via western blotting. * $P < 0.05$, ** $P < 0.01$ and *** $P < 0.001$. PVT1, plasmacytoma variant translocation 1; NLRP3, nucleotide-binding oligomerization domain-like receptor protein 3; LPS, lipopolysaccharide; LDH, lactate dehydrogenase; ASC, apoptosis-associated speck-like protein containing a CARD; sh, short hairpin RNA; NC, negative control.

compared with shNC, which demonstrated successful knockdown (Fig. 2A). The ELISA results demonstrated that the levels of IL-1 β , IL-18 and LDH were significantly increased in the LPS group compared with the control group, which was significantly reversed by transfection with shPVT1 compared with transfection with shNC (Fig. 2B-D). A similar trend was observed for the protein expression levels of NLRP3, IL-1 β , IL-18, ASC and cleaved caspase-1 (Fig. 2F). In addition, LPS significantly increased the percentage of active caspase-1-PI double-positive cells compared with the control group, whereas shPVT1 transfection reduced the LPS-induced cell pyroptosis rate compared with shNC transfection (Fig. 2E). The protein expression levels of cleaved-GSDME and active caspase-11 were not significantly altered by LPS treatment compared with the control group (Fig. S2). By contrast, the

expression of cleaved-GSDMD was significantly increased in LPS-induced HK-2 cells compared with control HK-2 cells. The results suggested that LPS-induced cell pyroptosis was caused by caspase-1, not caspase-11. In addition, PVT1 overexpression significantly promoted increased HK-2 cell pyroptosis compared with the vector group (Fig. S3). Collectively, the aforementioned results demonstrated that PVT1 knockdown inhibited cell pyroptosis in LPS-induced HK-2 cells.

PVT1 serves as a sponge of miR-20a-5p. Subsequently, the binding relationship between PVT1 and miR-20a-5p was verified. PVT1 localization tests were conducted, and the results demonstrated that most PVT1 molecules were located in the nucleus compared with the cytoplasm (Fig. 3A). starBase was used to predict the binding sites between PVT1 and miR-20a-5p,

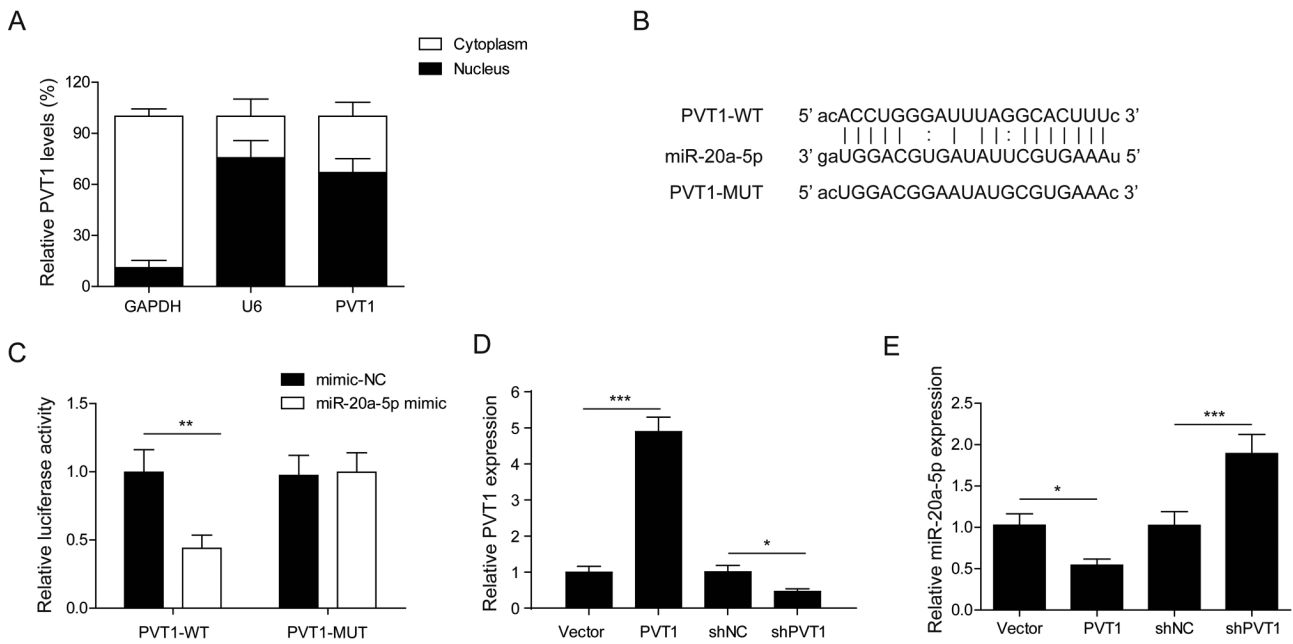


Figure 3. PVT1 serves as a sponge of miR-20a-5p. (A) PVT1 localization in HK-2 cells. (B) starBase was used to predict the sequence of the binding site between PVT1 and miR-20a-5p. (C) Dual luciferase reporter assays were performed to assess the direct binding of PVT1 to miR-20a-5p. (D) PVT1 and (E) miR-20a-5p expression levels in HK-2 cells were detected via reverse transcription-quantitative PCR. * $P < 0.05$, ** $P < 0.01$ and *** $P < 0.001$. PVT1, plasmacytoma variant translocation 1; miR, microRNA; WT, wild-type; MUT, mutant; NC, negative control; sh, short hairpin RNA.

and PVT1 3'UTR MUT was constructed (Fig. 3B). The dual luciferase reporter assay results indicated that compared with the mimic NC group, miR-20a-5p mimic significantly reduced the luciferase activity of PVT1-WT, but displayed no obvious effect on the luciferase activity of PVT1-MUT, verifying the direct binding of PVT1 and miR-20a-5p (Fig. 3C). Moreover, PVT1 overexpression significantly increased PVT1 expression and significantly decreased miR-20a-5p expression compared with the vector group (Fig. 3D and E). By contrast, PVT1 knockdown significantly decreased PVT1 expression and significantly increased miR-20a-5p expression compared with the shNC group. In summary, the results indicated that PVT1 served as a sponge of miR-20a-5p.

NLRP3 is a target gene of miR-20a-5p. Since PVT1 knockdown blocked NLRP3-mediated pyroptosis, the targeting relationship between miR-20a-5p and NLRP3 was investigated. First, the binding sites between miR-20a-5p and NLRP3 were predicted using starBase, and an NLRP3 3'UTR MUT was constructed (Fig. 4A). The dual luciferase reporter assay results indicated that compared with the mimic NC group, miR-20a-5p mimic significantly reduced the luciferase activity of NLRP3-WT, but did not significantly alter the luciferase activity of NLRP3-MUT, verifying the direct binding of NLRP3 and miR-20a-5p (Fig. 4B). Compared with the mimic NC group, miR-20a-5p mimic significantly increased miR-20a-5p expression levels, but significantly decreased NLRP3 mRNA and protein expression levels (Fig. 4C-E). By contrast, miR-20a-5p inhibitor significantly reduced miR-20a-5p expression, and significantly increased NLRP3 mRNA and protein expression levels compared with the inhibitor NC group. Overall, the results indicated that miR-20a-5p targeted NLRP3 and negatively regulated NLRP3 expression.

PVT1 promotes NLRP3-mediated pyroptosis via miR-20a-5p in LPS-induced HK-2 cells. PVT1, miR-20a-5p and NLRP3 knockdown experiments were conducted to explore the mechanism underlying PVT1-mediated promotion of pyroptosis in septic AKI. First, the knockdown effect of siNLRP3 was verified, and the results demonstrated that transfection of siNLRP3 effectively reduced NLRP3 expression (Fig. S4). Compared with the control group, LPS significantly decreased miR-20a-5p expression. Compared with the LPS group, LPS + shPVT1 significantly increased miR-20a-5p expression, but LPS + miR-20a-5p inhibitor significantly decreased miR-20a-5p expression. However, co-transfection with shPVT1 and miR-20a-5p significantly recovered miR-20a-5p expression levels (Fig. 5A). Compared with the control group, LPS significantly enhanced NLRP3 mRNA and protein expression levels. Compared with the LPS group, LPS + shPVT1 significantly decreased NLRP3 mRNA and protein expression levels, but LPS + miR-20a-5p inhibitor significantly increased NLRP3 mRNA and protein expression levels. Moreover, co-transfection with miR-20a-5p inhibitor and shPVT1 or siNLRP3 significantly recovered NLRP3 mRNA and protein expression levels (Fig. 5B and G). Similar trends were observed for the levels of IL-1 β , IL-18 and LDH (Fig. 5C-E), and the protein expression levels of NLRP3, IL-1 β , IL-18, ASC and cleaved caspase-1 (Fig. 5G). Compared with the control group, LPS significantly increased the cell pyroptosis rate, but shPVT1 significantly inhibited LPS-induced cell pyroptosis (Fig. 5F). In addition, miR-20a-5p inhibitor significantly enhanced LPS-induced cell pyroptosis. In LPS-treated + miR-20a-5p inhibitor-transfected cells, transfection with shPVT1 or siNLRP3 significantly reversed miR-20a-5p inhibitor-mediated effects. The results indicated that PVT1 regulated NLRP3 via miR-20a-5p to promote the pyroptosis of LPS-induced HK-2 cells.

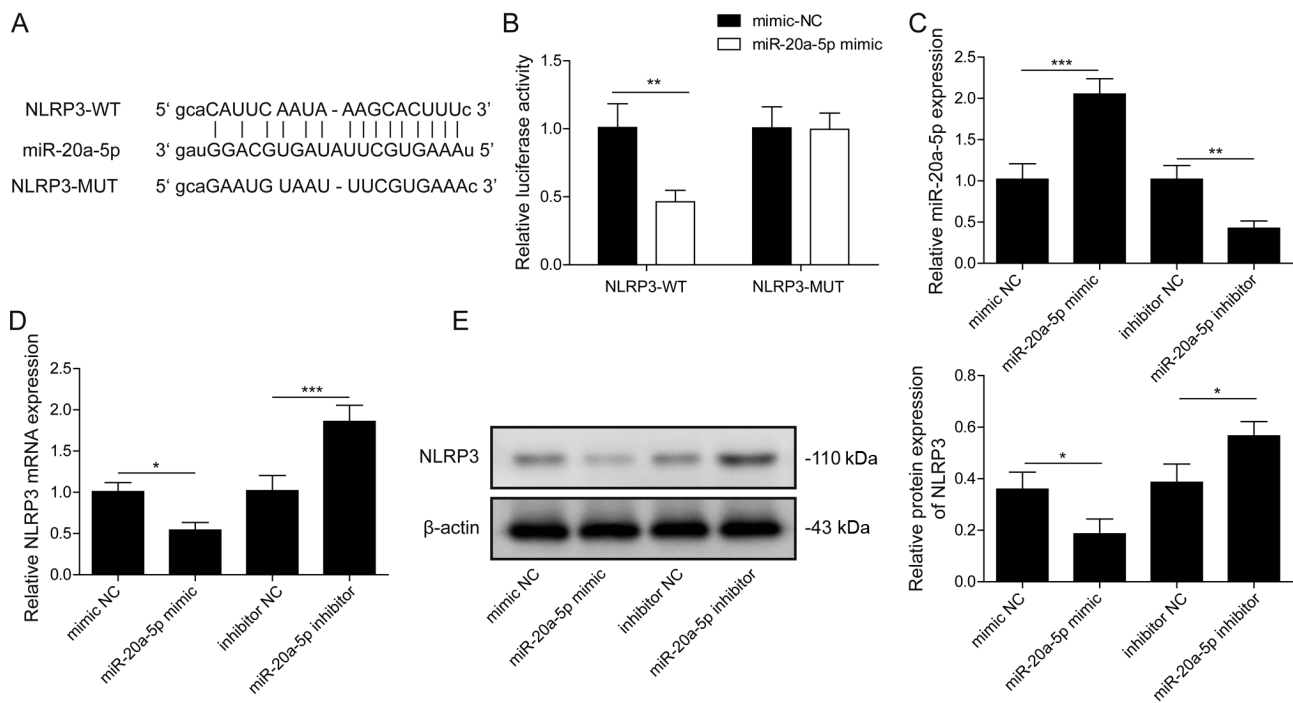


Figure 4. NLRP3 is a target gene of miR-20a-5p. (A) starBase was used to predict the sequence of the binding site between miR-20a-5p and NLRP3. (B) Dual luciferase reporter assays were performed to assess the direct binding of miR-20a-5p to NLRP3. (C) miR-20a-5p and (D) NLRP3 expression levels were detected via reverse transcription-quantitative PCR. (E) NLRP3 protein expression levels were measured via western blotting. * $P < 0.05$, ** $P < 0.01$ and *** $P < 0.001$. NLRP3, nucleotide-binding oligomerization domain-like receptor protein 3; miR, microRNA; WT, wild-type; MUT, mutant; NC, negative control.

Discussion

Sepsis is an acute systemic inflammatory response caused by infection that is characterized by the excessive release of various inflammatory mediators, causing extensive cell and tissue damage (18). The kidney is the most vulnerable organ for the development of sepsis (19,20). The secretion of inflammatory factors, which trigger cell pyroptosis, are key aspects of the pathogenesis of endotoxaemia and sepsis (21). Ye *et al* (22) reported that caspase-11-induced tubular epithelial cell pyroptosis was a key event during septic AKI, and inhibition of cell pyroptosis might serve as a key event against septic AKI (22). Therefore, the present study investigated the regulatory mechanism underlying cell pyroptosis in septic AKI.

Increasing evidence has demonstrated that lncRNAs serve major roles in the pathogenesis of septic AKI (7). In the present study, lncRNA PVT1 expression was significantly increased in the kidney tissues of septic AKI model mice and a septic AKI cell model compared with sham mice and control HK-2 cells, respectively. PVT1 was reported to be an oncogenic lncRNA that is highly expressed in a variety of malignancies and is associated with poor prognosis (23). More importantly, PVT1 was reported to be highly expressed in septic AKI, and PVT1 promoted septic AKI by upregulating the inflammatory response (5). Moreover, Huang *et al* (7) indicated that PVT1 can promote LPS-induced septic AKI via the regulation of TNF- α and JNK/NF- κ B signalling pathways in HK-2 cells. The aforementioned studies indicate that PVT1 is closely related to the development of septic AKI; however, the role of lncRNA PVT1 in regulating cell pyroptosis in septic AKI has not been previously reported. In the present study, compared with shNC, PVT1 knockdown significantly decreased LPS-induced

HK-2 cell pyroptosis. The results indicated that PVT1 might enhance cell pyroptosis in septic AKI; thus, the mechanism underlying PVT1-mediated regulation of pyroptosis in septic AKI was investigated.

The lncRNA/miRNA axis has a large regulatory effect on the process of several diseases (24,25). For example, lncRNA small nucleolar RNA host gene 3 can enhance the invasion and migration of osteosarcoma by downregulating miRNA-151a-3p expression (25). miRNAs participate in numerous biological processes, and research demonstrates that miRNAs serve important roles in sepsis (26,27). Specifically, miRNAs, including miRNA-21 and miRNA-23a, can protect against sepsis-induced tissue damage (26,27). The present study verified a binding site for miR-20a-5p in PVT1. miR-20a-5p was reported to serve a vital role in the occurrence of septic AKI (28), and a previous study suggested that miR-20a-5p was downregulated in septic AKI (29). The results of the present study indicated that PVT1 served as a sponge of miR-20a-5p to aggravate LPS-induced pyroptosis by inhibiting miR-20a-5p function. Therefore, it was concluded that PVT1 regulated cell pyroptosis in septic AKI by mediating miR-20a-5p.

miRNAs may bind to the 3'UTR of their target genes to regulate inflammation (28). The results of the present study demonstrated that miR-20a-5p contained a binding site to a protein complex that serves a crucial role in pyroptosis, NLRP3. NLRP3 is the most widely studied inflammasome and belongs to the family of NLR proteins (30). Activated NLRP3 binds with ASC, which contains a pyrin domain (PYD) and a caspase-recruitment domain (CARD), via PYD interaction. Moreover, the CARD of ASC recruits pro-caspase-1 to the complex (31). The present study

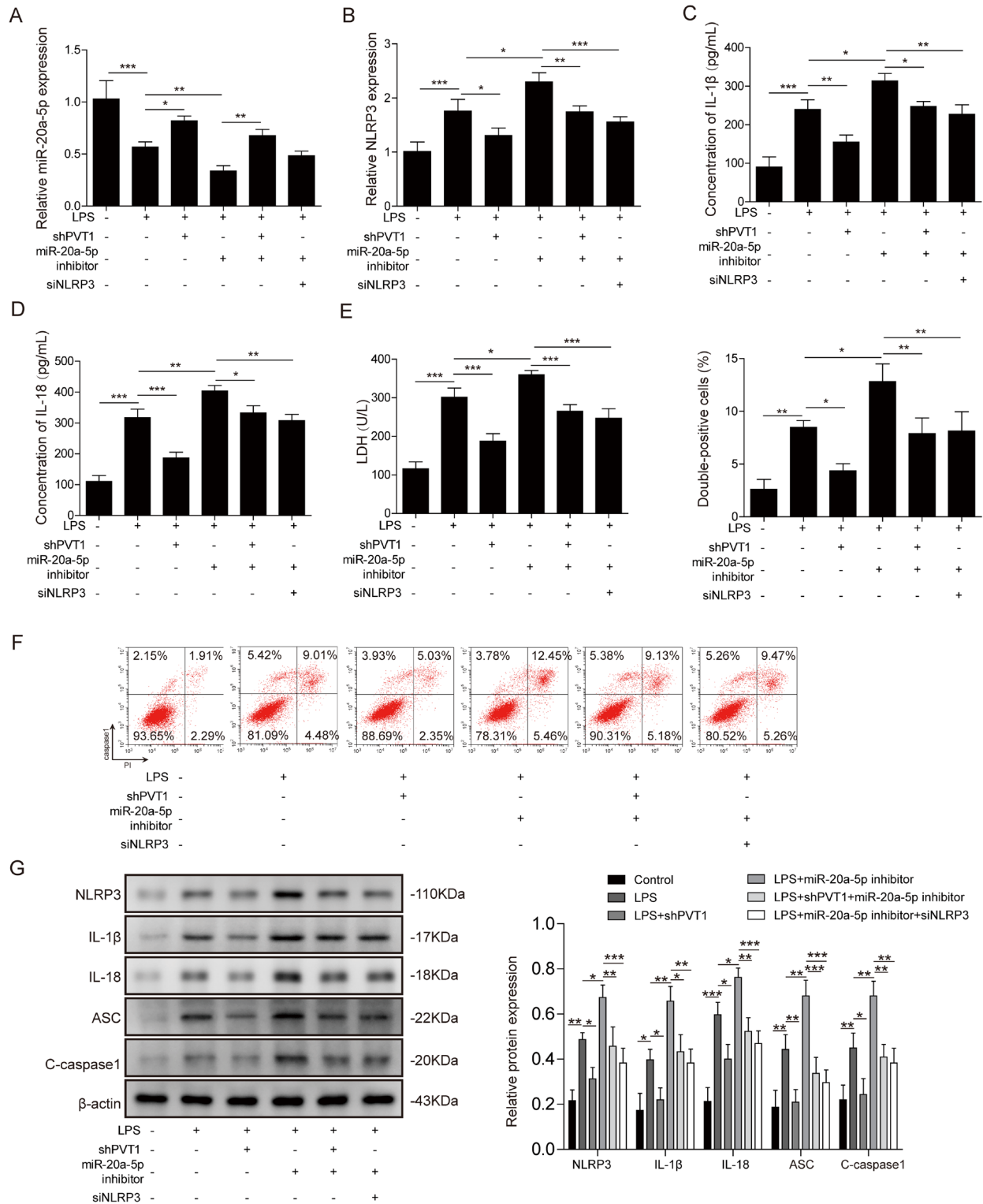


Figure 5. PVT1 promotes NLRP3-mediated pyroptosis via miR-20a-5p in LPS-induced HK-2 cells. (A) miR-20a-5p and (B) NLRP3 expression levels were detected via reverse transcription-quantitative PCR. (C) IL-1 β and (D) IL-18 levels were detected by performing ELISAs. (E) LDH secretion was measured using an LDH cytotoxicity assay kit. (F) Cell pyroptosis was detected via flow cytometry. (G) NLRP3, IL-1 β , IL-18, ASC and cleaved caspase-1 protein expression levels were measured via western blotting. * $P < 0.05$, ** $P < 0.01$ and *** $P < 0.001$. PVT1, plasmacytoma variant translocation 1; NLRP3, nucleotide-binding domain-like receptor protein 3; miR, microRNA; LPS, lipopolysaccharide; LDH, lactate dehydrogenase; ASC, apoptosis-associated speck-like protein containing a CARD; sh, short hairpin RNA; si, small interfering RNA.

also indicated that NLRP3 served an important role in the occurrence of pyroptosis in septic AKI, and PVT1 knockdown inhibited cell pyroptosis by regulating the miR-20a-5p/NLRP3 axis in septic AKI.

In conclusion, the present study identified a potential mechanism underlying PVT1-mediated regulation of pyroptosis in septic AKI. PVT1 modulated NLRP3-mediated pyroptosis via miR-20a-5p in septic AKI, which indicated the potential of

using PVT1 to treat septic AKI. Therefore, PVT1 might serve as a potential therapeutic target for septic AKI.

Acknowledgements

Not applicable.

Funding

The present study was supported by the National Natural Science Foundation of China (grant no. 81501710), the Scientific Research Project of Hunan Health Committee (grant no. B2019175) and the New Xiangya Talent Projects of the Third Xiangya Hospital of Central South University (grant no. JY201606).

Availability of data and materials

The datasets used and/or analysed during the current study are available from the corresponding author on reasonable request.

Authors' contributions

MG and LTD guaranteed the integrity of the entire study and confirmed the authenticity of the raw data, conceived the study and reviewed the manuscript. MG and LTD conceptualized and designed the study. LTD performed the literature research, acquired the data, and prepared and edited the manuscript. LTD and QLW performed the experiments. CY analysed the data. All authors read and approved the final manuscript.

Ethics approval and consent to participate

All procedures related to animal experiments were reviewed and approved by the Third Xiangya Hospital of Central South University [approval no. LLSC (LA)2018-030].

Patient consent for publication

Not applicable.

Competing interests

The authors declare that they have no competing interests.

References

- Singer M, Deutschman CS, Seymour CW, Shankar-Hari M, Annane D, Bauer M, Bellomo R, Bernard GR, Chiche JD, Cooper-Smith CM, *et al*: The third international consensus definitions for sepsis and septic shock (Sepsis-3). *JAMA* 315: 801-810, 2016.
- Chen RM, Chen T, Lin L, Chang C, Chang H and Wu C: Anti-inflammatory and antioxidative effects of propofol on lipopolysaccharide-activated macrophages. In: *The 2nd Conference of Asian Society for Mitochondrial Research and Medicine*. Taipei, Taiwan, 2004.
- Bagshaw SM, Uchino S, Bellomo R, Morimatsu H, Morgera S, Schetz M, Tan I, Bouman C, Macedo E, Gibney N, *et al*: Septic acute kidney injury in critically ill patients: Clinical characteristics and outcomes. *Clin J Am Soc Nephrol* 2: 431-439, 2007.
- Chen F, Liu M, Yu Y, Sun Y, Li J, Hu W, Wang X and Tong D: LINC00958 regulated miR-627-5p/YBX2 axis to facilitate cell proliferation and migration in oral squamous cell carcinoma. *Cancer Biol Ther* 20: 1270-1280, 2019.
- Huang W, Li X, Wang D, Sun Y, Wang Q, Bu Y and Niu F: Curcumin reduces LPS-induced septic acute kidney injury through suppression of lncRNA PVT1 in mice. *Life Sci* 254: 117340, 2020.
- Wang J, Song J, Li Y, Shao J, Xie Z and Sun K: Down-regulation of lncRNA CRNDE aggravates kidney injury via increasing MiR-181a-5p in sepsis. *Int Immunopharmacol* 79: 105933, 2020.
- Huang W, Lan X, Li X, Wang D, Sun Y, Wang Q, Gao H and Yu K: Long non-coding RNA PVT1 promote LPS-induced septic acute kidney injury by regulating TNF α and JNK/NF- κ B pathways in HK-2 cells. *Int Immunopharmacol* 47: 134-140, 2017.
- Bhatt K, Mi QS and Dong Z: microRNAs in kidneys: Biogenesis, regulation, and pathophysiological roles. *Am J Physiol Renal Physiol* 300: F602-F610, 2011.
- Bartel DP: MicroRNAs: Target recognition and regulatory functions. *Cell* 136: 215-233, 2009.
- Lamkanfi M and Dixit VM: Inflammasomes and their roles in health and disease. *Annu Rev Cell Dev Biol* 28: 137-161, 2012.
- Wang IK, Sun KT, Tsai TH, Chen CW, Chang SS, Yu TM, Yen TH, Lin FY, Huang CC and Li CY: MiR-20a-5p mediates hypoxia-induced autophagy by targeting ATG16L1 in ischemic kidney injury. *Life Sci* 136: 133-141, 2015.
- Anders HJ: Of inflammasomes and alarmins: IL-1 β and IL-1 α in kidney disease. *J Am Soc Nephrol* 27: 2564-2575, 2016.
- Wen Y, Liu YR, Tang TT, Pan MM, Xu SC, Ma KL, Lv LL, Liu H and Liu BC: mROS-TXNIP axis activates NLRP3 inflammasome to mediate renal injury during ischemic AKI. *Int J Biochem Cell Biol* 98: 43-53, 2018.
- Komada T, Usui F, Kawashima A, Kimura H, Karasawa T, Inoue Y, Kobayashi M, Mizushima Y, Kasahara T, Taniguchi S, *et al*: Role of NLRP3 inflammasomes for rhabdomyolysis-induced acute kidney injury. *Sci Rep* 5: 10901, 2015.
- Liang F, Zhang F, Zhang L and Wei W: The advances in pyroptosis initiated by inflammasome in inflammatory and immune diseases. *Inflamm Res* 69: 159-166, 2020.
- Livak KJ and Schmittgen TD: Analysis of relative gene expression data using real-time quantitative PCR and the 2(-Delta Delta C(T)) method. *Methods* 25: 402-408, 2001.
- Otero-Antón E, González-Quintela A, López-Soto A, López-Ben S, Llovo J and Pérez LF: Cecal ligation and puncture as a model of sepsis in the rat: Influence of the puncture size on mortality, bacteremia, endotoxemia and tumor necrosis factor alpha levels. *Eur Surg Res* 33: 77-79, 2001.
- Martin GS: Sepsis, severe sepsis and septic shock: Changes in incidence, pathogens and outcomes. *Expert Rev Anti Infect Ther* 10: 701-706, 2012.
- Zarjou A and Agarwal A: Sepsis and acute kidney injury. *J Am Soc Nephrol* 22: 999-1006, 2011.
- Bellomo R, Kellum JA, Ronco C, Wald R, Martensson J, Maiden M, Bagshaw SM, Glassford NJ, Lankadeva Y, Vaara ST and Schneider A: Acute kidney injury in sepsis. *Intensive Care Med* 43: 816-828, 2017.
- Shi J, Zhao Y, Wang K, Shi X, Wang Y, Huang H, Zhuang Y, Cai T, Wang F and Shao F: Cleavage of GSDMD by inflammatory caspases determines pyroptotic cell death. *Nature* 526: 660-665, 2015.
- Ye Z, Zhang L, Li R, Dong W, Liu S, Li Z, Liang H, Wang L, Shi W, Malik AB, *et al*: Caspase-11 mediates pyroptosis of tubular epithelial cells and septic acute kidney injury. *Kidney Blood Press Res* 44: 465-478, 2019.
- Tang J, Li Y, Sang Y, Yu B, Lv D, Zhang W and Feng H: lncRNA PVT1 regulates triple-negative breast cancer through KLF5/beta-catenin signaling. *Oncogene* 37: 4723-4734, 2018.
- Wang JY, Yang Y, Ma Y, Wang F, Xue A, Zhu J, Yang H, Chen Q, Chen M, Ye L, *et al*: Potential regulatory role of lncRNA-miRNA-mRNA axis in osteosarcoma. *Biomed Pharmacother* 121: 109627, 2020.
- Zheng S, Jiang F, Ge D, Tang J, Chen H, Yang J, Yao Y, Yan J, Qiu J, Yin Z, *et al*: lncRNA SNHG3/miRNA-151a-3p/RAB22A axis regulates invasion and migration of osteosarcoma. *Biomed Pharmacother* 112: 108695, 2019.
- Yang J, Mao M and Zhen YY: miRNA-23a has effects to improve lung injury induced by sepsis in vitro and vivo study. *Biomed Pharmacother* 107: 81-89, 2018.
- Fu D, Dong J, Li P, Tang C, Cheng W, Xu Z, Zhou W, Ge J, Xia C and Zhang Z: MiRNA-21 has effects to protect kidney injury induced by sepsis. *Biomed Pharmacother* 94: 1138-1144, 2017.

28. Brandenburger T, Salgado Somoza A, Devaux Y and Lorenzen JM: Noncoding RNAs in acute kidney injury. *Kidney Int* 94: 870-881, 2018.
29. Ge QM, Huang CM, Zhu XY, Bian F and Pan SM: Differentially expressed miRNAs in sepsis-induced acute kidney injury target oxidative stress and mitochondrial dysfunction pathways. *PLoS One* 12: e0173292, 2017.
30. Yu ZW, Zhang J, Li X, Wang Y, Fu YH and Gao XY: A new research hot spot: The role of NLRP3 inflammasome activation, a key step in pyroptosis, in diabetes and diabetic complications. *Life Sci* 240: 117138, 2020.
31. Hoss F, Rodriguez-Alcazar JF and Latz E: Assembly and regulation of ASC specks. *Cell Mol Life Sci* 74: 1211-1229, 2017.